arXiv:1509.02210v1 [astro-ph.EP] 7 Sep 2015

WASP-120 B, WASP-122 B AND WASP-123 B: THREE NEWLY DISCOVERED PLANETS FROM THE WASP-SOUTH SURVEY

O.D.Turner[1], D. R. Anderson[1], A. Collier Cameron[2], L. Delrez[3], M. Gillon[3], C. Hellier[1], E. Jehin[3], M. Lendl[4], P. F. L. Maxted[1], F. Pepe[5], D. Pollacco[6], D. Queloz[7], D. Ségransan[5], B. Smalley[1], A. M. S. Smith[8,9], A. H. M. J. Triaud[5,10,11], S. Udry[5], R. G. West[6]

Draft version September 9, 2015

ABSTRACT

We present the discovery by the WASP-South survey of three planets transiting moderately bright stars (V ≈ 11). WASP-120 b is a massive ($5.0M_{\rm Jup}$) planet in a 3.6-day orbit that we find likely to be eccentric ($e = 0.059^{+0.025}_{-0.018}$) around an F5 star. WASP-122 b is a hot-Jupiter ($1.37M_{\rm Jup}$, $1.79R_{\rm Jup}$) in a 1.7-day orbit about a G4 star. Our predicted transit depth variation caused by the atmosphere of WASP-122 b suggests it is well suited to characterisation. WASP-123 b is a hot-Jupiter ($0.92M_{\rm Jup}$, $1.33R_{\rm Jup}$) in a 3.0-day orbit around an old (~ 7 Gyr) G5 star.

Subject headings: Planetary systems — stars: individual (WASP-120,WASP-122,WASP-123)

1. INTRODUCTION

The Wide Angle Search for Planets (WASP) survey is a prolific contributor to the field of exoplanet science having published the discovery of 104 planets to date. Our effective magnitude range of $9 < V < 13$ means that WASP systems are conducive to further study. Examples from the extremes of this range are the bright WASP-33 (V = 8.3; Collier Cameron et al. 2010) and WASP-18 (V = 9.3; Hellier et al. 2009) and the relatively dim WASP-112 (V = 13.3; Anderson et al. 2014).

Here we present the discovery of: WASP-120 b, a system with a star showing variable activity and a possibly eccentric planet orbit, WASP-122 b, which offers a good opportunity for atmospheric study, and WASP-123 b, which orbits an old star, ~ 7 Gyr.

2. OBSERVATIONS

The transits of these planets were discovered in photometry gathered from the WASP-South installation hosted by the South African Astronomical Observatory. The WASP-South instrument is an array of 8 cameras using 200mm $f/1.8$ lenses to survey the sky at a cadence of ~ 10 minutes. For more information on the

TABLE 1
Observations of WASP-120, WASP-122 and WASP-123

Date	Source	N.Obs. / Filter	Comment
WASP-120			
2006 Aug–2012 Jan	WASP-South	27 079	
2013 Sep–2015 Mar	CORALIE	29	
2013 Nov 12	TRAPPIST	I+z	Meridian flip
2014 Aug 17	EulerCam	$I_{\rm c}$	
2014 Dec 07	EulerCam	$I_{\rm c}$	
WASP-122			
2011 Oct–2012 Mar	WASP-South	4 834	
2013 Nov–2014 Oct	CORALIE	17	
2013 Dec 17	TRAPPIST	z	Meridian flip
2014 Jan 15	TRAPPIST	z	Slight cloud
2014 Jan 15	EulerCam	r	Slight cloud
2014 Jan 22	EulerCam	r	Slight cloud
WASP-123			
2006 May–2012 Jun	WASP-South	13 267	
2013 Sep–2014 Aug	CORALIE	20	
2014 Sep 06	EulerCam	z	
2014 Sep 06	TRAPPIST	$I_{\rm c}$	
2014 Sep 09	TRAPPIST	z	

WASP instrument, see Pollacco et al. (2006). The data were processed and searched for transits as described in Collier Cameron et al. (2006) with candidate selection following the procedure in Collier Cameron et al. (2007a). Details of observations for each star in this paper can be found in Table 1. The phase-folded WASP data are displayed in the top panels of Figs. 1, 2 and 3. We used the method of Maxted et al. (2011) to search the WASP photometry for modulations caused by star spots. We detected no rotational modulation above 2 mmag which suggests that the hosts are inactive.

We obtained spectra of the three stars with the CORALIE spectrograph on the 1.2-m Swiss telescope as outlined in Table 1. We used these data to measure radial velocity (RV) variations and confirm the planetary nature of the candidates (Table 2; bottom panel of Figs. 1, 2 and 3). We obtained 9 of the WASP-120 spectra after the spectrograph was upgraded in November 2014. The lack of correlation between the bisector spans and RVs (Fig. 4) indicate that the RV variations are not a result of blended eclipsing binaries.

We acquired the follow-up photometry needed to accu-

[1] Astrophysics Group, Keele University, Staffordshire ST5 5BG, UK
[2] SUPA, School of Physics and Astronomy, University of St. Andrews, North Haugh, Fife KY16 9SS, UK
[3] Institut d'Astrophysique et de Géophysique, Universitè de Liége, Allèe du 6 Août, 17, Bat. B5C, Liège 1, Belgium
[4] Austrian Academy of Sciences, Space Research Institute, Schmiedlstrae 6, 8042 Graz, Austria
[5] Observatoire de Genève, Université de Genève, 51 Chemin des Maillettes, 1290 Sauverny, Switzerland
[6] Department of Physics, University of Warwick, Coventry CV4 7AL, UK
[7] Cavendish Laboratory, J J Thomson Avenue, Cambridge, CB3 0HE, UK
[8] N. Copernicus Astronomical Centre, Polish Academy of Sciences, Bartycka 18, 00-716, Warsaw, Poland
[9] Institute of Planetary Research, German Aerospace Center, Rutherfordstrasse 2, D-12489 Berlin, Germany
[10] Centre for Planetary Sciences, University of Toronto at Scarborough, Toronto, Ontario M1C 1A4, Canada
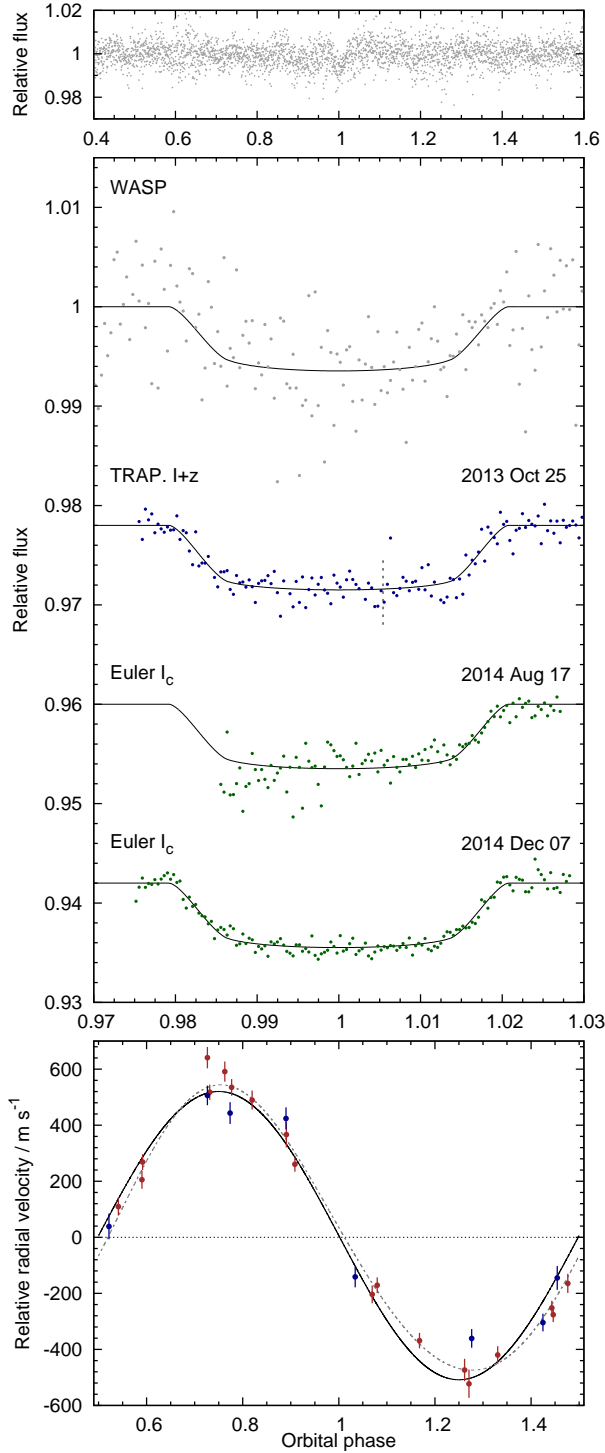[11] Department of Astronomy & Astrophysics, University of Toronto, Toronto, ON M5S 3H4, Canada

FIG. 1.— Discovery data for WASP-120 b. *Top panel:* Phase folded WASP photometry for WASP-120. *Middle panel:* WASP discovery photometry (grey), TRAPPIST (blue) and EulerCam (green) follow-up photometry with best fit transit model overplotted. The meridian flip in the TRAPPIST data has been corrected for and marked with a vertical dashed line. All photometric data have been binned with a duration of 2 minutes for clarity. *Bottom panel:* CORALIE radial velocity data from before (red) and after (blue) the upgrade, over-plotted with the best fit circular (black-solid) and eccentric (grey-dashed) solutions.
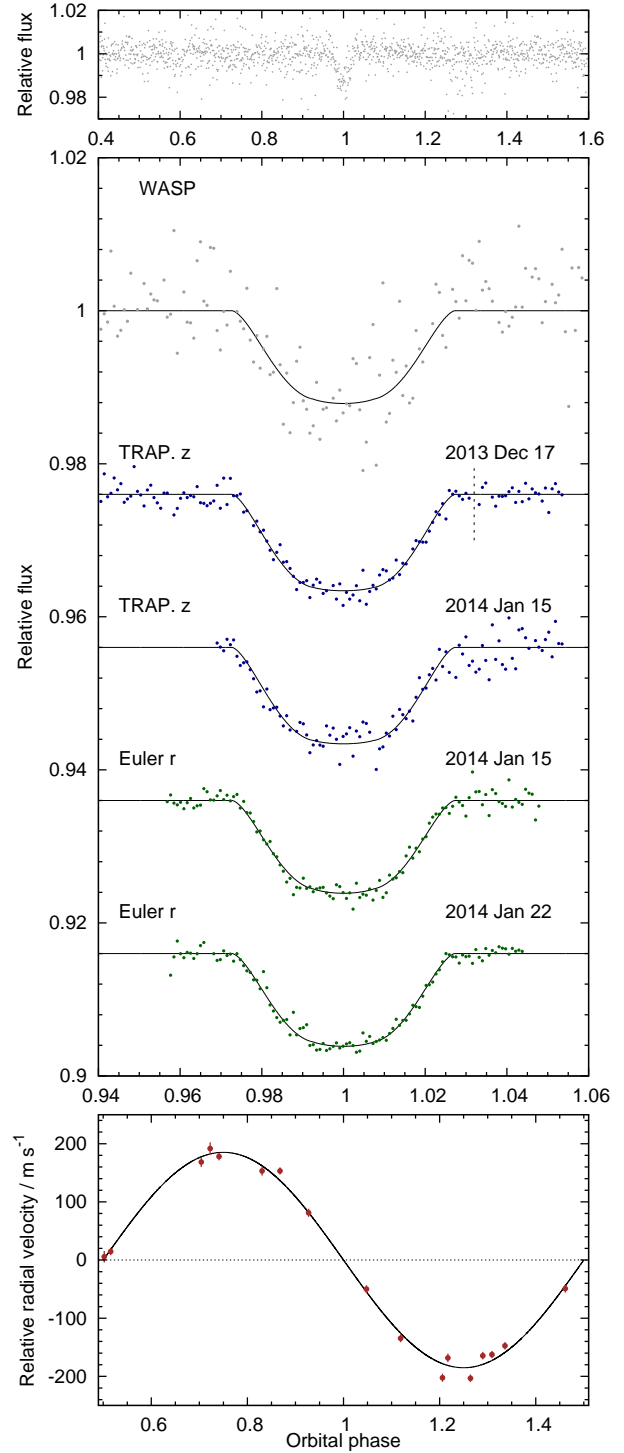
FIG. 2.— Discovery data for WASP-122 b. *Top panel:* Phase folded WASP photometry for WASP-122. *Middle panel:* WASP discovery photometry (grey), TRAPPIST (blue) and EulerCam (green) follow-up photometry with best fit transit model overplotted. The meridian flip in the TRAPPIST data has been corrected for and marked with a vertical dashed line. All photometric data have been binned with a duration of 2 minutes for clarity. *Bottom panel:* CORALIE radial velocity data, over-plotted with the best fit circular solution.
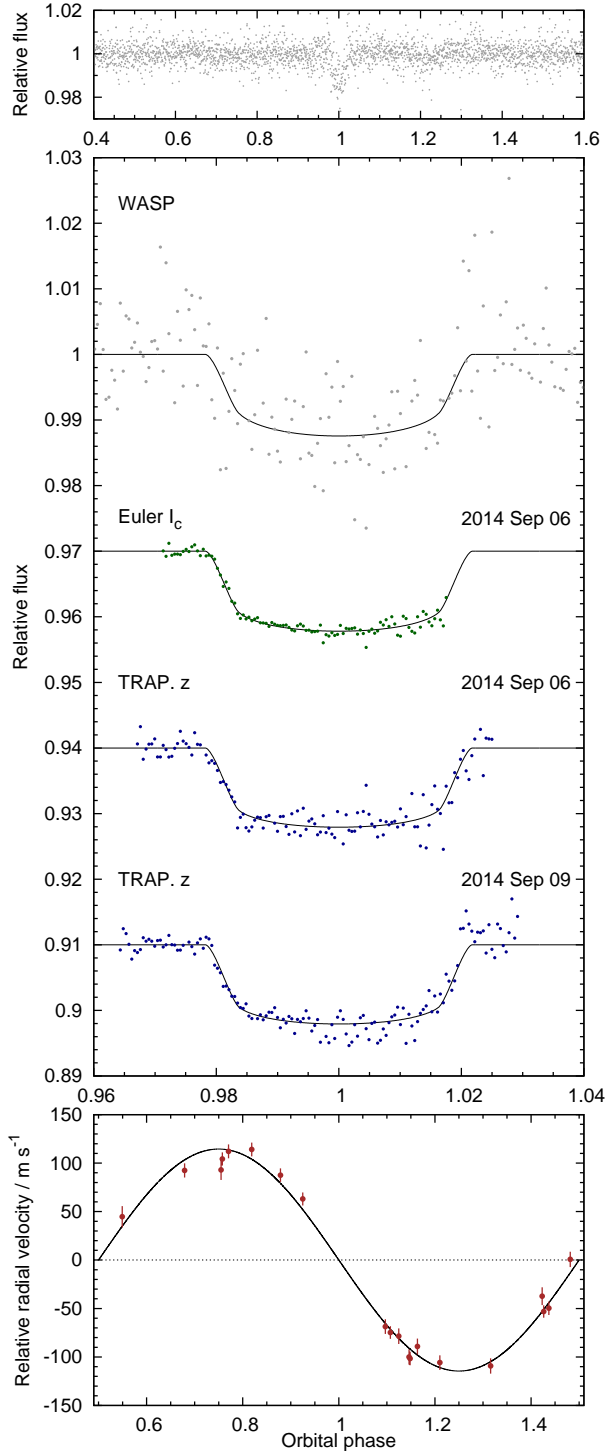
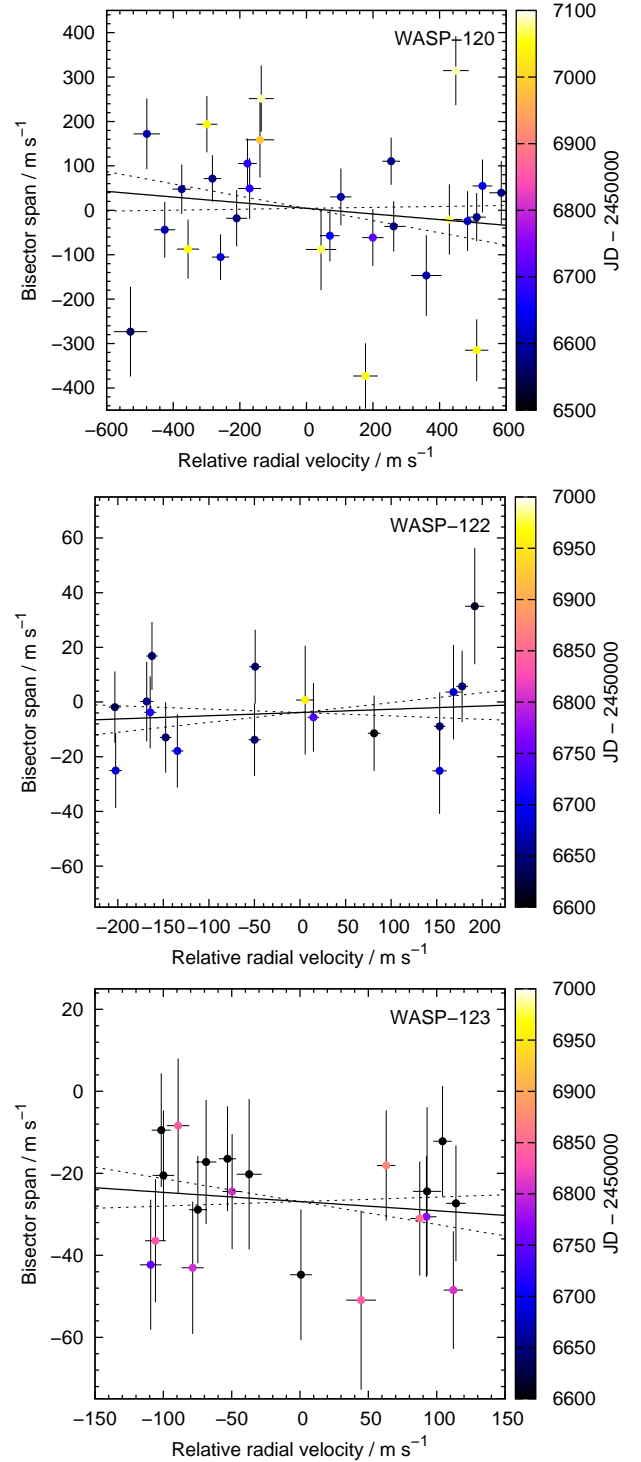Fig. 3.— Discovery data for WASP-123 b. Caption as for Fig. 2.

Fig. 4.— Bisector spans plotted against relative radial velocities for WASP-120 (top), WASP-122 (middle) and WASP-123 (bottom) showing no correlation. Solid lines are results of least-squares fits to the data, dashed lines are the 1σ uncertainties of the fits. Date of observation is denoted by point colour. The increased dispersion of points seen in more recent data for WASP-120 is attributed to an increase in stellar activity.

rately determine the system parameters from the 0.6-m TRAPPIST telescope (Gillon et al. 2011) and EulerCam (Lendl et al. 2012) on the Swiss telescope at La Silla, Chile. The TRAPPIST telescope's equatorial mount requires a meridian flip when the target culminates during an observation. These occurred at BJD = 2456609.725 during the transit of WASP-120 on 2013 Nov 12 and at BJD = 2456644.758 during the transit of WASP-122 on 2013 Dec 17. We account for any offsets introduced by

TABLE 2
RADIAL VELOCITY DATA FROM CORALIE.

HJD − 2 540 000	RV (km s^{-1})	Error (km s^{-1})	BS (km s^{-1})	Target Name
6552.902673	19.30305	0.05043	−0.27331	WASP-120
6572.735422	20.41666	0.03569	0.03952	WASP-120
6573.843533	19.62205	0.03173	−0.01785	WASP-120
...	...	...	...	...
...	...	...	...	...
6871.746191	16.99747	0.00673	−0.01808	WASP-123

NOTE. — Data available in this format at ADS. The data are provided to the full precision used in our calculations but times are only accurate to a few seconds at best.

treating them as two separate datasets during our analysis. The photometric data are presented in Table 3.

3. ANALYSIS

3.1. *Stellar Parameters*

We determined the atmospheric parameters of each host star by analysing the co-added CORALIE spectra after correcting them for shifts due to the radial motion of the star using the measured RVs. Our spectral analysis followed procedures given in Doyle et al. (2013). For each star we obtained the effective temperature, $T_{\rm eff}$, using the Hα line, $\log g$ from the Na D and Mg b lines and iron abundances from the analysis of equivalent width measurements of several unblended Fe I lines. We found the projected rotation velocity, $V \sin i$, by fitting the profiles of the Fe I lines after convolving with the instrumental resolution ($R = 55\,000$) and a macroturbulent velocity adopted from the calibration of Doyle et al. (2014). The results of our analysis can be found in the top part of Table 4.

3.2. *System Parameters*

We used a Markov chain Monte Carlo (MCMC) code to determine the system parameters using the discovery and follow-up photometry with RVs as described by Collier Cameron et al. (2007b) and Anderson et al. (2015).

We modelled our transit lightcurves using the formulation of Mandel & Agol (2002) and accounted for limb-darkening using the four-parameter non-linear law of Claret (2000, 2004). We determined the mean stellar density, ρ_s, from the transit lightcurves and used the empirical mass calibration by Southworth (2011a) as a constraint on the stellar mass allowing us to derive the corresponding mass and radius of the planet.

The free parameters in our MCMC analysis were T_0, P, $(R_P/R_s)^2$, T_{14}, b, K_1, γ, $T_{\rm eff}$ and [Fe/H]. Here T_0 is the epoch of mid-transit, P, is the orbital period, $(R_P/R_s)^2$ is the planet-to-star area ratio, T_{14} is the total transit duration, b is the impact parameter of the planet's path across the stellar disc, K_1 is the reflex velocity semi-amplitude, γ is the systemic velocity, $T_{\rm eff}$ is the stellar effective temperature and [Fe/H] is the stellar metallicity. We placed priors on both $T_{\rm eff}$ and [Fe/H] using the values derived from the analysis of the spectra (Section 3.1). When we allow the MCMC to explore eccentric solutions we fit $\sqrt{e}\cos\omega$ and $\sqrt{e}\sin\omega$ to ensure a uniform probability distribution. We present the results for each system in the lower part of Table 4.

4. WASP-120

WASP-120 b is a 5.0-$M_{\rm Jup}$, 1.5-$R_{\rm Jup}$ planet orbiting a moderately bright ($V = 11.0$) F5 star. The effective temperature of WASP-120 places it in the lithium gap (Böhm-Vitense 2004), so we cannot estimate the age of this star based on the lithium abundance. Using the star's Tycho B−V colour and rotation period from its $V \sin i$ and radius from our MCMC we use gyrochronology calibration of Barnes (2007) to estimate an age of 0.7 ± 0.6 Gyr. For comparison, the calibration of Mamajek & Hillenbrand (2008) gives 1.0 ± 1.8 Gyr. We used BAGEMASS (Maxted et al. 2015) to compare the observed values of [Fe/H], $T_{\rm eff}$ and ρ_s to stellar models in order to estimate the age and mass of WASP-120. We find an age of 2.6 ± 0.5 Gyr and a stellar mass of 1.39 ± 0.06 $M_\odot$ which is in good agreement with our analysis. The age is consistent with that of the Mamajek & Hillenbrand calibration.

The FWHM of the lines in the spectra and the bisector spans show more scatter in the later data, after the CORALIE upgrade (Fig. 5), suggesting that the star may have become more active, and therefore have variable activity like the Sun and WASP-111 (Anderson et al. 2014). Similar behaviour to this was seen with the RVs of WASP-111, though its RVs were all obtained before the upgrade.

Due to the upgrade to CORALIE we partitioned the data into two sets. We added jitter of 5.1 ms^{-1} to the older data and 6.3 ms^{-1} to the newer data. These values were adopted such that both datasets gave reduced χ^2 values of one compared to a circular-orbit solution, and are in keeping with jitter determined for similar stars by Wright (2005)

The best-fitting solution had an eccentricity of $0.059^{+0.025}_{-0.018}$. This is significantly non-zero at 3.3σ, while a Lucy-Sweeny test (Lucy & Sweeney 1971) gives a probability of only 0.1% that the orbit is circular. We note, though, that this result is somewhat dependent on the jitter values used. Fitting with no jitter increased the best fitting eccentricity to 0.068 ± 0.014. This led to a higher apparent significance (4.9σ) though the Lucy-Sweeny test no longer excluded the circular solution. As planets of this mass often have an eccentric orbit we choose to accept this solution for WASP-120 b (Fig 1).

Notable examples of massive planets with confidently detected eccentricities are HAT-P-16 b (Buchhave et al. 2010), HAT-P-21 b (Bakos et al. 2011), WASP-14 b (Joshi et al. 2009) and WASP-89 b (Hellier et al. 2014). All of these are in sub 7-day orbits with masses $> 4M_{\rm Jup}$. Also notable are HAT-P-20 b (Bakos et al. 2011), which has the smallest eccentricity of the group and Kepler-14 b with the longest orbital period at 6.79-days (Buchhave et al. 2011).

A conclusive determination of this system's eccentricity would come from observation of an occultation which we expect to be delayed by 2.6 ± 1.1 hours if our eccentricity value is accurate. Based on the equilibrium temperature of the planet, we estimate occultation depths in the *Spitzer* 3.6 μm and 4.5 μm bands of approximately 780 and 960 ppm, respectively. Recent observations with *Spitzer* (Zhao et al. 2014; Deming et al. 2015) show detecting such an occultation is easily achievable.

HJD$_{UTC}$ − 2 540 000	Norm. Flux	Error	ΔX Position	ΔY Position	Airmass	Target FWHM	Sky Bkg. (Counts)	Exp. Time (s)	Target Name	Instrument	Band
6887.720753	0.990347	0.002159	−1.91	−2.21	2.64	11.12	71.30	50.00	WASP-120	EulerCam	IC
6887.721534	0.996407	0.002145	0.25	−1.40	2.62	12.18	70.00	50.00	WASP-120	EulerCam	IC
6887.722324	0.994713	0.002114	0.06	−1.04	2.60	10.85	68.82	50.00	WASP-120	EulerCam	IC
...	...	...	...	...	...	...	...	...	...	...	...
...	...	...	...	...	...	...	...	...	...	...	...
6910.766640	0.992689	0.008096	−0.92	−0.64	2.91	4.08	293.86	13.00	WASP-123	TRAPPIST	z

Note. — Data available in this format at ADS. The data are provided to the full precision used in our calculations but times are only accurate to a few seconds at best.
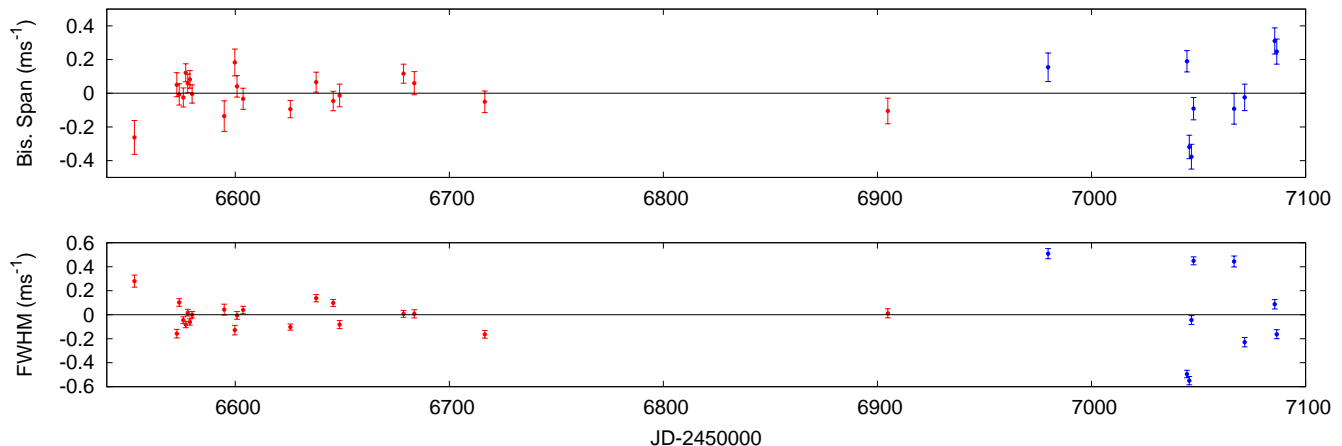

Fig. 5.— Full width at half-maximum (FWHM) and bisector spans of spectra as a function of time for WASP-120. The increase in scatter in more recent data is taken as an indication the star may be entering a phase of increased activity. In red are data taken before the CORALIE upgrade and in blue are those taken after. The data have all had the mean of their distribution subtracted before plotting.
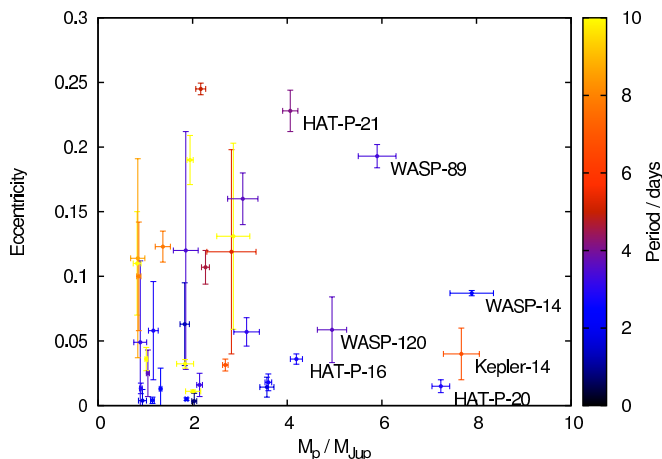

Fig. 6.— Masses, eccentricities and periods of transiting planets with non-zero eccentricities quoted in literature and masses > $0.5M_{Jup}$ mass. The most convincing eccentricities are those associated with more massive planets. Notable examples and WASP-120 b are labelled. Data from TEPCat (Southworth 2011b).

5. WASP-122

WASP-122 b is a $1.37M_{Jup}$, $1.79R_{Jup}$ planet orbiting a moderately bright (V = 11.0), metal rich ([Fe/H] = +0.32 ± 0.09), G4 star. WASP-122 is depleted in lithium ($\log A(Li) < 1.0$) and so must be several Gyr old (Sestito & Randich 2005). Using the star's colour and rotational period from its $V \sin i$, we calculate a gyrochronological age of 2.3 ± 1.4 Gyr (Barnes 2007).

The calibrations of Mamajek & Hillenbrand (2008) and Meibom et al. (2009) suggest a similar age. Using bage-mass we find two possible solutions. Approximately 75% of the Markov chain output by bagemass favour a mass of 1.24 ± 0.04 $M_\odot$ and an age of 5.11 ± 0.80 Gyr. The mass from this solution agrees with that found by our MCMC to within 1σ. The other 25% of the output prefer a solution giving a mass of 1.10 ± 0.03 $M_\odot$ and an age of 8.67 ± 1.05 Gyr. The favoured, younger, higher-mass solution is a better match to the gyrochronological age and MCMC mass.

WASP-122 b presents a good target for atmospheric characterisation via transmission spectroscopy. Assuming the atmosphere is isothermal and adequately described as an ideal gas we predict a transit depth variation due to one atmospheric scale height of 142 ppm. The same calculation for the well-studied HD 209458 b yields a variation of ≈ 200 ppm. Deming et al. (2013) found evidence for water absorption on this scale in HD 209458 b. While WASP-122 is dim by comparison to HD 209458 constraints have been put on the atmospheric compositions of planets with similarly bright hosts e.g. WASP-12 (V = 11.6, Sing et al. 2013; Kreidberg et al. 2015).

We predict occultation depths in 3.6 μm and 4.5 μm Spitzer bands of 2100 and 2500 ppm respectively. In the K-band we predict a depth of 1000 ppm. Similar K-band depths have been detected, for example that of WASP-10 b (Cruz et al. 2015), making ground-based follow up possible.

6. WASP-123

WASP-123 b is a 0.92-$M_{\rm Jup}$, 1.33-$R_{\rm Jup}$ planet orbiting a moderately bright (V = 11.1), G5 star with a super-solar metal abundance ([Fe/H] = $+0.18 \pm 0.08$). WASP-123 is depleted in lithium ($\log A(Li) < 0.5$) suggesting an age of several Gyr. This star falls into an area of parameter space for which gyrochronology is poorly calibrated (Jeffries 2014). The Barnes calibration gives an age greater than the present age of the universe and Mamajek and Meibom calibrations are not applicable due to the star's colour. The age we derive using BAGEMASS, 6.9 ± 1.4 Gyr, supports this. The mass we find with BAGEMASS, $1.17 \pm 0.06\ M_\odot$, is in good agreement with our analysis. Planets of similar mass and radius are not uncommon and are frequently found in orbits $\sim$ 3-days around such host stars. This makes WASP-123 a typical example of a hot-Jupiter system.

REFERENCES

Anderson, D. R., Brown, D. J. A., Collier Cameron, A., et al. 2014, ArXiv e-prints, arXiv:1410.3449
Anderson, D. R., Collier Cameron, A., Hellier, C., et al. 2015, A&A, 575, A61
Bakos, G. Á., Hartman, J., Torres, G., et al. 2011, ApJ, 742, 116
Barnes, S. A. 2007, ApJ, 669, 1167
Böhm-Vitense, E. 2004, AJ, 128, 2435
Buchhave, L. A., Bakos, G. Á., Hartman, J. D., et al. 2010, ApJ, 720, 1118
Buchhave, L. A., Latham, D. W., Carter, J. A., et al. 2011, ApJs, 197, 3
Claret, A. 2000, A&A, 363, 1081
—. 2004, A&A, 428, 1001
Collier Cameron, A., Pollacco, D., Street, R. A., et al. 2006, MNRAS, 373, 799
Collier Cameron, A., Wilson, D. M., West, R. G., et al. 2007a, MNRAS, 380, 1230
—. 2007b, MNRAS, 380, 1230
Collier Cameron, A., Guenther, E., Smalley, B., et al. 2010, MNRAS, 407, 507
Cruz, P., Barrado, D., Lillo-Box, J., et al. 2015, A&A, 574, A103
Deming, D., Wilkins, A., McCullough, P., et al. 2013, ApJ, 774, 95
Deming, D., Knutson, H., Kammer, J., et al. 2015, ApJ, 805, 132
Doyle, A. P., Davies, G. R., Smalley, B., Chaplin, W. J., & Elsworth, Y. 2014, MNRAS, 444, 3592
Doyle, A. P., Smalley, B., Maxted, P. F. L., et al. 2013, MNRAS, 428, 3164
Gillon, M., Jehin, E., Magain, P., et al. 2011, in European Physical Journal Web of Conferences, Vol. 11, European Physical Journal Web of Conferences, 6002
Hellier, C., Anderson, D. R., Collier Cameron, A., et al. 2009, Nature, 460, 1098
—. 2014, ArXiv e-prints, arXiv:1410.6358
Jeffries, R. D. 2014, in EAS Publications Series, Vol. 65, EAS Publications Series, 289–325
Joshi, Y. C., Pollacco, D., Collier Cameron, A., et al. 2009, MNRAS, 392, 1532
Kreidberg, L., Line, M. R., Bean, J. L., et al. 2015, ArXiv e-prints, arXiv:1504.05586
Lendl, M., Anderson, D. R., Collier-Cameron, A., et al. 2012, A&A, 544, A72
Lucy, L. B., & Sweeney, M. A. 1971, AJ, 76, 544
Mamajek, E. E., & Hillenbrand, L. A. 2008, ApJ, 687, 1264
Mandel, K., & Agol, E. 2002, ApJL, 580, L171
Maxted, P. F. L., Serenelli, A. M., & Southworth, J. 2015, A&A, 575, A36
Maxted, P. F. L., Anderson, D. R., Collier Cameron, A., et al. 2011, PASP, 123, 547
Meibom, S., Mathieu, R. D., & Stassun, K. G. 2009, ApJ, 695, 679
Pollacco, D. L., Skillen, I., Collier Cameron, A., et al. 2006, PASP, 118, 1407
Sestito, P., & Randich, S. 2005, A&A, 442, 615
Sing, D. K., Lecavelier des Etangs, A., Fortney, J. J., et al. 2013, MNRAS, 436, 2956
Southworth, J. 2011a, MNRAS, 417, 2166
—. 2011b, MNRAS, 417, 2166
Wright, J. T. 2005, PASP, 117, 657
Zhao, M., O'Rourke, J. G., Wright, J. T., et al. 2014, ApJ, 796, 115

TABLE 4
Stellar and planetary parameters parameters determined from spectra and MCMC analysis.

Spectroscopic Parameter	WASP-120	WASP-122	WASP-123
Tycho-2 ID	8068-01208-1	7638-00981-1	7427-00581-1
USNO-B ID	0441-0033568	0475-0113097	0571-1147509
RA (J2000)	04:10:27.85	07:13:12.34	19:17:55.04
Dec (J2000)	-45:53:53.5	-42:24:35.1	-32:51:35.8
V Magnitude	11.0	11.0	11.1
Tycho (B$-$V) colour	0.523 ± 0.083	0.78 ± 0.11	0.48 ± 0.17
Spectral Type	F5	G4	G5
Stellar Effective Temperature, $T_{\rm eff}$ (K)	6450 ± 120	5720 ± 130	5740 ± 130
Stellar Surface Gravity, $\log g_{\rm s}$	4.3 ± 0.1	4.3 ± 0.1	4.3 ± 0.1
Stellar Metallicity, [Fe/H]	-0.05 ± 0.07	0.32 ± 0.09	0.18 ± 0.08
Projected Rot. Vel., $V \sin i$ (km s^{-1})	15.1 ± 1.2	3.3 ± 0.8	1.0 ± 0.7
Stellar Lithium Abundance, $\log A$(Li)	< 1.2	< 1.0	< 0.5
Micro turbulence (km s^{-1})	1.5 ± 0.1	0.9 ± 0.1	1.0 ± 0.1
Macro turbulence (km s^{-1})	6.0 ± 0.8	3.4 ± 0.5	3.4 ± 0.5
MCMC Parameter	WASP-120	WASP-122	WASP-123
Period, P (d)	3.6112706 ± 0.0000038	1.7100567 ± 0.0000036	2.9776410 ± 0.0000024
Transit Epoch, T_0	6779.43520 ± 0.00044	6665.22403 ± 0.00022	6845.17081 ± 0.00041
Transit Duration, T_{14} (d)	0.1479 ± 0.0016	0.0910 ± 0.0009	0.1288 ± 0.0015
Scaled Semi-major Axis, a/R_s	5.81 ± 0.21	4.262 ± 0.077	7.16 ± 0.24
Transit Depth, $(R_p/R_s)^2$	0.00652 ± 0.00016	0.01383 ± 0.00029	0.01107 ± 0.00027
Impact Parameter, b	0.780 ± 0.021	0.8608 ± 0.0073	$0.525^{+0.041}_{-0.053}$
Orbital Inclination, i ($^\circ$)	82.29 ± 0.48	78.35 ± 0.31	85.79 ± 0.51
Eccentricity (adopted), e	$0.059^{+0.025}_{-0.018}$	0	0
Eccentricity (limit), e (at 2σ)	$-$	< 0.08	< 0.12
Argument of Periastron, ω ($^\circ$)	-37^{+39}_{-21}	$-$	$-$
Systemic Velocity, γ (kms^{-1})	19.836 ± 0.014	34.5934 ± 0.0017	16.9344 ± 0.0017
Semi-amplitude, K_1 (ms^{-1})	511.3 ± 9.2	185.2 ± 2.3	114.5 ± 2.3
Semi-major Axis, a (au)	0.0522 ± 0.0013	0.03107 ± 0.00079	0.0431 ± 0.0011
Stellar Mass, M_s ($M_\odot$)	1.45 ± 0.11	1.4 ± 0.1	1.207 ± 0.089
Stellar Radius, R_s ($R_\odot$)	1.93 ± 0.09	1.567 ± 0.051	1.296 ± 0.061
Stellar Density, ρ_s ($\rho_\odot$)	0.202 ± 0.022	0.355 ± 0.019	0.554 ± 0.057
Stellar Surface Gravity, $\log(g_s)$ (cgs)	4.029 ± 0.031	4.184 ± 0.018	4.294 ± 0.029
Stellar Effective Temperature, $T_{\rm eff}$ (K)	6450 ± 120	5730 ± 130	5730 ± 130
Stellar Metallicity, [Fe/H]	-0.052 ± 0.072	0.319 ± 0.089	0.181 ± 0.075
Planet Mass, M_p ($M_{\rm Jup}$)	5.01 ± 0.26	1.372 ± 0.072	0.92 ± 0.05
Planet Radius, R_p ($R_{\rm Jup}$)	1.515 ± 0.083	1.792 ± 0.069	1.327 ± 0.074
Planet Density, ρ_p ($\rho_{\rm Jup}$)	1.44 ± 0.21	$0.237^{+0.023}_{-0.018}$	0.395 ± 0.056
Planet Surface Gravity, $\log(g_p)$ (cgs)	3.70 ± 0.04	2.989 ± 0.024	3.079 ± 0.039
Planet Equilibrium Temperature, $T_{\rm eq}$ (K)	1890 ± 50	1960 ± 50	1510 ± 40